Design and Fabrication of A Dielectric Antenna for Millimeter-Wave Wireless Applications.

Loka Elkess[1, *], Ashraf A. M. Khalaf[1], N. M. Rashad[1,2]

[1]*Communications and Electronics Engineering Department, Faculty of Engineering, Minia University, Minia, Egypt.*

[2]*Communications and Electronics Engineering Department, Faculty of Engineering, October University for Modern Sciences and Arts (MSA), Giza Egypt.*

* corresponding author E-mail: lokanoos@yahoo.com

ABSTRACT

In this paper, three different designs of antenna structures suitable for millimeter-wave applications have been proposed, simulated, and fabricated to meet the desired criteria of future wireless technologies. The effects of varying ground plane dimensions and structures (DGS) over cylindrical dielectric resonators (CDRs) for achieving compact-wideband-multi-resonating frequency antennas have been considered. The first proposed antenna is a two-element CDRs of Rogers RT/Duroid 6010LM mounted on a low-cost FR-4 surface, which enhances the antenna's ability to operate at frequency bands (2 -2.8) GHz, (5.7-7.2) GHz, (9.7-10.8) GHz, and (13.4-14.3) GHz. The second proposed antenna is capable of operating in four different frequency bands: (2.5-3.7) GHz, (7.8-8.5) GHz, (10.5-12) GHz, and (14.6–15.9) GHz. The final proposed antenna permits the antenna to operate in broader and higher frequency bands (6.8–7.8) GHz and (10.5–35) GHz with a fractional bandwidth of 14% and 76.8%, respectively. The reflection coefficient is below -10 dB for all the mentioned frequency bands. All results were simulated using Microwave Studio Software (**CST)** and **High-Frequency Simulator Structure (HFSS).** The third proposed antenna was fabricated and compared the measuring results to the related simulation results. This compact-sized antenna has fractional bandwidth, appropriate gain, and a stable radiation pattern over the operating frequency bands. Making it suitable for use in 5G, WiMAX, C-band, X-band, Ku-band, and millimeter-wave (MM-W) wireless applications. Moreover, the proposed antennas are suitable for future sub-6 GHz band applications.

Keywords: Compact Dielectric Resonator Antenna (CDRA), Defected ground structure (DGS), reflection coefficient, fractional bandwidth, Millimeter-wave(MM-W), Sub-6 GHz band.

I. INTRODUCTION

The wireless communication industry has grown significantly, and the evolution of communication never stops. With this rapid growth, the need for improved antenna features such as antenna size, traffic demand, high data rate, bandwidth, gain, and efficiency is challenging for researchers. New wireless applications such as millimeter-wave are required to overcome existing issues such as slow data rate and spectrum scarcity [1]. Antenna designs are fundamental to fulfilling all the requirements of modern technologies [2]. The microstrip patch antenna at high frequencies has low radiation, limited gain, and narrow bandwidths due to the inherent metal losses.

In contrast, S. A. Long first carried out the resonator antenna in 1983 to overcome many antenna deficiencies [3]. Dielectric Resonator Antennas (DRAs) offer many advantages such as high radiation efficiency, ease of excitation, low dissipation loss, low cost, temperature stability, and cover wide frequency band (0.7-35) GHz [4][14]. Dielectric resonator antennas let engineers dream for the next generation of wireless communication applications [5].

Getting to millimeter-wave frequency (mm-w) bands that extend from30 – 300 GHz with high-speed wireless connectivity for future 5G communications, tracking; such as

compact radar systems [6]. on the 24th of April 2020, FCC (Federal Communications Commission) opened a 6-GHz band (5.925-7.125 GHz) for unlicensed indoor devices allowing 5.925-6.425 GHz and 6.525-6.875 GHz sub-bands for unlicensed point-to-point devices transmitting indoors and outdoors with low power levels [7]. Thus, FCC expanded the Mid-band spectrum and allowed the use of the band between 3.7 – 24 GHz for Wi-Fi and other unlicensed applications.

Many miniaturization techniques have been recently used to reduce antenna sizes, such as using short pins, increasing current path lengths, split-ring resonator, high-permittivity dielectric, and defect ground structural (DGS) modification [25]. DGS technology can also produce an acceptable multiband by cutting different shapes of slots in the ground plane. DGS has a simple and wide range of applications in microwave circuit designs, including filters, amplifiers, and oscillators[8]. Dielectric Resonator Antennas (DRAs) can also reduce antenna sizes. Using Cylindrical DRA (CDRA), additional advantages are ease of fabrication and the ability to exciting different modes [17]. The formula to calculate the resonant frequency of a CDRA [9] is

$$F_r = \frac{c}{\pi D \sqrt{\varepsilon_{DRA}}} \left[1.71 + \frac{D}{2H} + 0.1578 \left(\frac{D}{2H}\right)^2 \right] \quad [1]$$

Where D and H are the diameter and height, respectively, of the CDRA and is the relative permittivity of the material, the above expression is only valid for hybrid mode, and the same dielectric resonator antenna can be excited by using

different modes, i.e., TE and TM modes but calculated with different resonant frequency expressions.

Fast and new technologies encourage researchers to find and develop better solutions for wireless applications with compact and cheap designs to meet the market needs.

TABLE I. Comparison between recently published DRA designs

Ref.	Antenna Dimensions (mm)	DR ε_r	Num of DRs	Frequency (GHz)	BW	Peak Gain (dBi)
[10]	60 x 45 x 19	2.2	2	4.8-9.66	67.5 %	N/A
[11]	16 x 8.5 x 11.6	9.6	1	3.1-12.1	N/A	unstable
[14]	33 x 38 x 7.524	10	3	2.54-3.22, 4.06-5.04, 6.04-13.64	137 %	5.9
[15]	N/A x N/A x 3.9	6 , 7	2	26.9	25.1 - 30.1	6.5
[24]	60 x 60 10.508	10	1	3.85 , 7.85	10 %, 10 %	6.26

Table I shows a comparison of related work recently published of DRAs where the last three references used CDRAs. All these antennas cannot be easily fabricated due to their design complexity however, the maximum achieved gain in only 6.26 dBi and the operated bandwidth is relatively not enough to fulfill the market demand.

In this paper, an antenna design with CDRs and three different ground structures are presented and discussed, gaining the advantage of wide bandwidth and compact size to meet the criterion of using sub-6 GHz and mid-band wireless applications. The most enhanced performance antenna (third design) contains two "C" slots in its ground structure which permits the antenna to operate in a wide bandwidth range allowing the use of millimeter-wave bands. Two compact Cylindrical Dielectric Resonators (CDRs) made up of RogersRT/Duroid 6010LM with dielectric constant 10.2 had been used as the main radiator in the proposed design. The CDRs are mounted on-FR4 substrate (4.4) and a "C" shaped feeding structure. It operates in different frequency bands ranging from 5to 35 GHz enhancing the use of Sub-6 GHz and MM-wave applications. All simulation results were performed using CST Microwave Studio (CST MWS) and High-Frequency Simulator Structure (HFSS) simulation tools showing good agreement between the simulated and measured results. The organization of the paper is as follows; section 2 presents the dielectric resonator antenna designs and the different ground structures and dimensions of each, section 3 discusses the parametric study that was carried out on some parameters and how these affect the spectrum, section 4 analyses the different partial ground effects on the dielectric resonator antenna discussing the measured and simulated results of the antennas in details, last but not least, section 5 presents the conclusion of the paper.

II. Antenna Designs

The three proposed designs have the exact physical dimensions of the overall antenna and the patch structure, each with different ground structures. Table II shows all the antenna parameters. The main antenna dimensions are Ls x Ws (50 mm x 50 mm) with height, Hs=1.6 mm of the substrate material Fire Redundant Epoxy (FR4) of dielectric constant = 4.4 and loss tangent $tan\delta$= 0.02.

TABLE II. Physical dimensions of the proposed antenna (mm)

Parameter	Value (mm)	Parameter	Value (mm)
Feeding line width, W_F	2.5	Feeding line length, L_F	19.5
Radiator outer diameter, D_{F1}	10.8	Radiator inner diameter, D_{F2}	8.8
Radiator thickness, T_F	2	CDR separation distance, X	20
CDR diameter, D	7	CDR thickness (RT 6010), H	2
Antenna height (FR4), Hs	1.6	Ground width, W_G	50

As shown in fig. 1, the main radiating element is a C-shape with an outer diameter, DF1, inner diameter, DF2, and an optimized length to meet the desired frequency band. The C-shape element is centered at the end of the 50Ω feeding line at length Lf and width Wf.

(a)   (b)
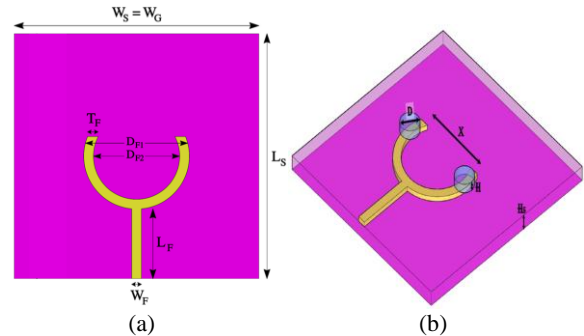
Fig. 1. Schematic diagram of the proposed antennas; (a) Microstrip Radiator, (b) 3D view.

Two Cylindrical Dielectric Resonators (CDRs) with diameter D are located above the C-shape radiating element at a height, H, of Rogers RT/duroid6010LM dielectric material with = 10.2 and tanδ = 0.0023. The two CDRs are separated with distance X.

As mentioned before, this paper discusses the effect of different ground structures, having the same radiating elements, on the resonating frequency bands. The following sections will discuss three different ground structures with the same main antenna structure and their effect on the bandwidth.

a. First Antenna Design

Fig. 2 shows the first proposed design with a partial ground structure of length, LG=16.6mm, and all physical dimensions are the same.
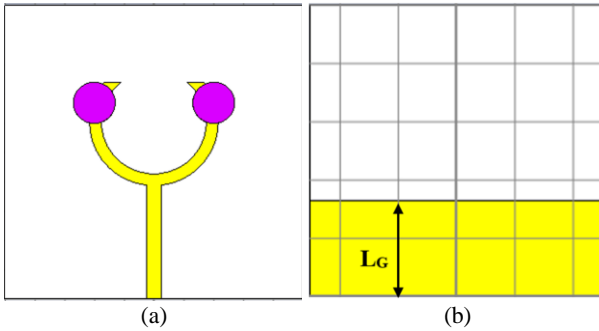
Fig. 2. Schematic diagram of the first antenna; (a) top view, (b)bottom view.

b. Second Antenna Design

In the second proposed design, the ground length, LG, has been changed from 16.6 mm to 19.6 mm, which the antenna's ability to work in different frequency bands, as will be discussed later. Fig. 3 shows the schematic diagram of the second antenna.
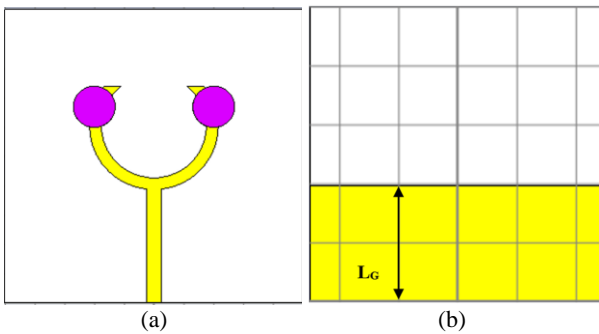
Fig. 3. Schematic diagram of the second antenna; (a) top view, (b)bottom view.

c. Third Antenna Design

As shown in Fig. 4, this design also has the same antenna parameter but with defected ground structure (DGS). The ground length, L_G, is changed to 50 mm with two "C" shapes mirrored to each other at a distance S = 2 mm and each with thickness C = 2 mm and their position was optimized to achieve the required bandwidth with the maximum gain and low plastic capacitance.
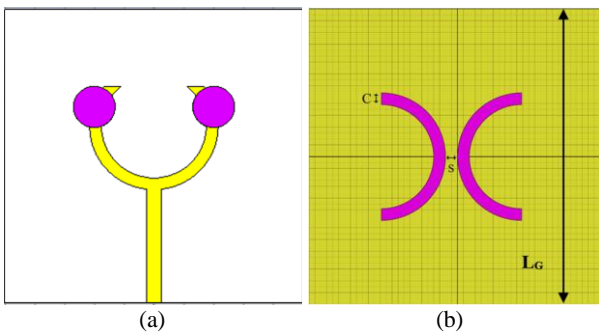
Fig. 4. Schematic diagram of the third antenna; (a) top view, (b) bottom view.

To achieve the parameters of these antennas getting the best performance. Many parameters were considered and optimized, and this study is discussed in the following section.

III. Parametric Analysis

antenna designs have passed through different optimization procedures using CST and HFSS simulators. The main target was to achieve wide bandwidth supporting the bands from 2 GHz to 35 GHz with multi-resonating frequencies and high gain compared to the existing ones. The main antenna radiator parameters were kept fixed. The optimization was carried on to study the effect of different ground structures with and without dielectric resonators on the antenna bandwidth. The results of this study are discussed below.
.

a. Effect of Different Ground Lengths

Fig. 5 shows the effect of different ground lengths, LG, for the same antenna structure with the CDRs on top of the radiator. It is seen that the first and second antennas operate in the band between 2 GHz to 16 GHz with different resonating frequencies, while the full Grounded antenna has a wide bandwidth with return loss below -10 dB from 21 GHz to 35 GHz.
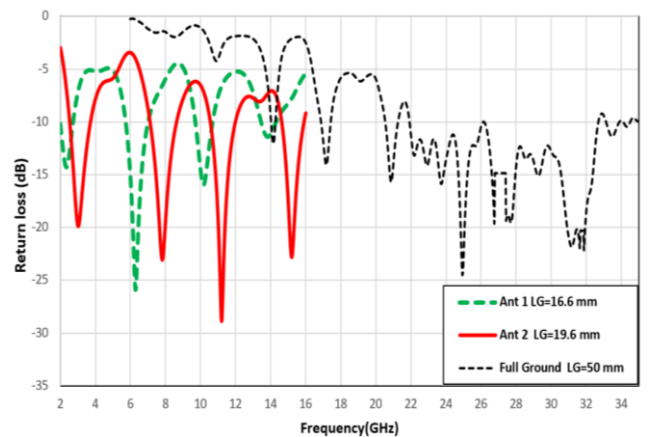
Fig. 5. Effect of different ground lengths on CDRA return loss.

Since the defected ground structures (DGSs) resulted in multi-resonant frequencies while the full ground structure resulted in a broad operating spectrum, we decided to study the effect of cutting slots in a full ground plane.

b. Effect of C-shape Slot in Full Ground Plane

Two C-shape slots were centered on the full ground plane of the CDR antenna having the same thickness (C = 2 mm and S = 2 mm) of the C-shape of the radiating element. Fig. 6 below shows how the antenna return loss changed, and the operating spectrum increased with this defected ground structure.
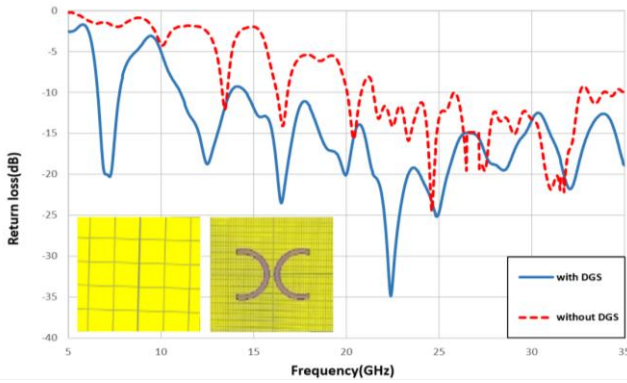
Fig. 6. Simulated return loss of the CDRA with and without two C-shapes ground slots.

TABLE III. Comparison of return losses at different resonating frequencies for the CDRA with and without C-shape DGS

Antenna Ground Plane Structure	Resonant Frequency (GHz)	Bandwidth (GHz)	Return Loss (dB)
Antenna without DGS	13.4	0.1	-12
	24.6	4.5	-24
	31.7	6	-21
Antenna with DGS	7.2	1.1	-20
	12.5	2.5	-19
	22.4	21.4	-35

Table III shows the effect of two C-shapes slots in the full ground of the same CDRA where it is observed that the return loss of the whole spectrum has declined by more than -10 dB, which results in wider operating bandwidth for each resonating frequency. Optimized Position, radius, and separating distance of the two C-shapes slots in the ground plane were to reach the best performance, getting S = 2 mm and C = 2 mm. Results of different spacing and dimensions of the C-shape slots are discussed in the following parts.

c. Effect of Different Spacing, S, between C-shapes

The effect of spacing (S) between the two C-shaped ground slots on the antenna return loss using CDRs was studied, and the results of different spacing are shown in fig. 7 below.
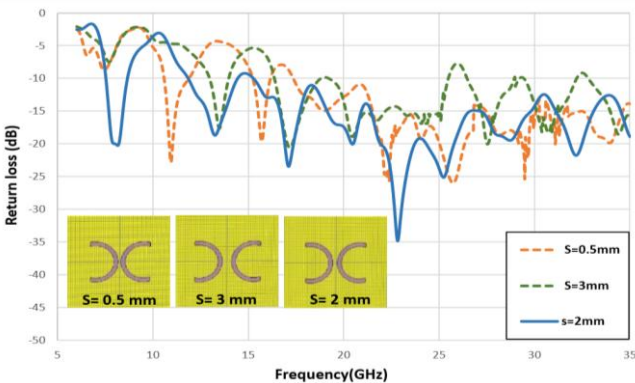
Fig. 7. Simulated return loss for three different spacing between two C-shape slots in ground plane of CDRA.

As seen in the above figure, almost all the simulated results of the three spacing between the two C-shape slots showed a broad operating spectrum at different resonating

frequencies. Also, it is observed that the large spacing, S = 3 mm, some

Band notches in the high frequencies (at 26 GHz, 29 GHz, and 32.5 GHz) can be optimized to meet their demanded applications. Table IV below shows the minimum return loss achieved for each spacing versus the resonating frequency.

TABLE IV. Minimum simulated return loss achieved for each spacing (S) versus the resonating frequency

Spacing between C-shapes	Resonant Frequency (GHz)	Return Loss (dB)
S = 0.5 mm	10.9	-23
S = 2 mm	22	-34
S = 3 mm	16	-23.5

As a result, the best performance is achieved at S = 2 mm. Other parameters are adjusted to achieve the best return loss while keeping the position of the two C-shape slots, the spacing (S) between them, and all other antenna parameters unchanged.

d. Effect of different C-shape ground slots radius

Moreover, studying the effect of different C-shape ground slot radiuses was very important. Fig. 8 below shows the simulated results of three different C-shape slot widths (C).
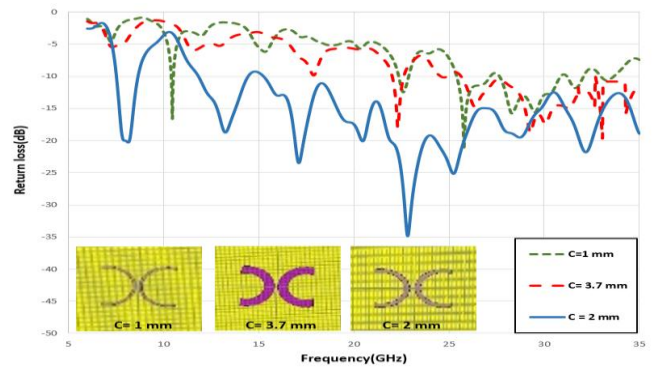
Fig. 8. Simulated return loss of different C-shape ground slot widths (C).

As seen in the above figure, the return loss of the very small and very big widths shows acceptable bandwidth in the range between 25 GHz to 35 GHz. Only while the width C = 2 mm shows a much wider operating bandwidth extending from 7 GHz to beyond 35 GHz with multi-resonating frequencies makes the antenna a perfect candidate for the required bandwidth. Table V below shows the minimum achieved return loss for each studied C-shape slot width versus the resonating frequency.

TABLE V. Minimum simulated return loss achieved for each C-shape slot width (C) versus the resonating frequency

C-shaped slots Width	Resonant Frequency (GHz)	Return Loss (dB)
C = 1.5 mm	10.5	-17
C = 2 mm	22.4	-35
C = 3.7 mm	21.5	-16

The optimization processes showed that the best bandwidth is achieved with S = 2 mm and C = 2 mm.

e. Effect of Dielectric Resonator

Last but not least, the effect of using dielectric material on top of the radiating element was studied, and fig. 9 below shows the return loss of the antenna with (using different diameters and thicknesses) and without using CDRs on top of the antenna. Two cylindrical dielectric materials of Rogers RT/duroid6010LM with thickness, H, and radius, D/2) are placed on top of the radiating element with separating distance, X. The position of the two CDRs and the distance between them were optimized by the simulators to achieve the best operating spectrum maintaining the radius to height ratio (D/2H) to be $0.5 \leq D/2H \leq 2$ to achieve multi-resonating frequencies [24]. Table VI shows a comparison between the return loss of some resonating frequencies for the designed C-shape ground slot antenna with and without CDRs on top of the radiating element.
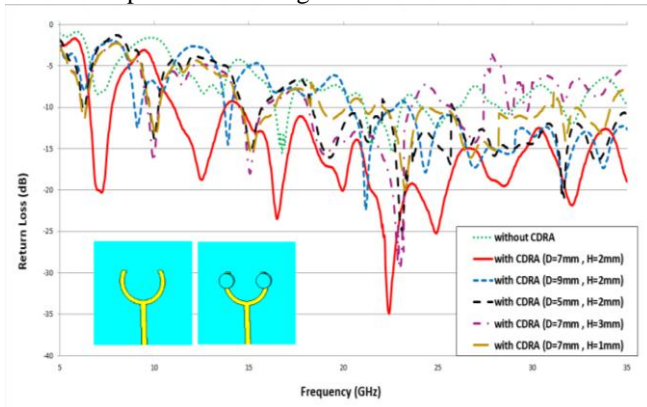
Fig. 9. Simulated return loss of the DGS antenna without CDRs and with CDRs using different diameter (D) and height (H).

TABLE VI. Comparison of return loss at different resonating frequencies with and without CDRs

Antenna Structure	Resonant Frequency (GHz)	Bandwidth (GHz)	Return Loss (dB)
Antenna with CDRA (D=7mm, H= 2mm)	7.2	1.1	-20
	12.5	2.5	-19
	22.4	21.4	-35
Antenna without CDRA	17	0.1	-15
	22.4	2	-15
	32.4	0.2	-12

It is observed that the return loss of both antennas, with and without CDRs, look similar with almost the same resonating frequencies but changing the diameters of the CDRs affected the return loss more than changing their heights. As seen in fig. 9, the best performance was achieved when D= 7mm and H= 2mm were used and made the return loss of the whole spectrum decline by about -20 dB compared to the return loss of the same antenna without using CDRs.

After the optimization process was done, three different designs were achieved, each serving different frequency

bands with high gain compared to those existing in the market. The simulation and fabrication results are discussed in the following section.

IV. Simulation and Fabrication Results

The main goal of this paper is to study the effect of defected ground structure (DGS) on compact dielectric resonators (CDR), permitting the antenna to work as a multiband millimeter-wave antenna. This section will discuss the simulated results of the three proposed antennas as well as the fabrication and measuring results of the third purposed antenna.

a. First Antenna Results

Fig. 10 shows the return loss over the frequency curve of the first antenna design where the operating frequency bands are from 2 GHz to 2.8 GHz, 5.7 GHz to 7.2GHz, 9.7 GHz to 10.8 GHz, and 13.4 GHz to 14.3 GHz.
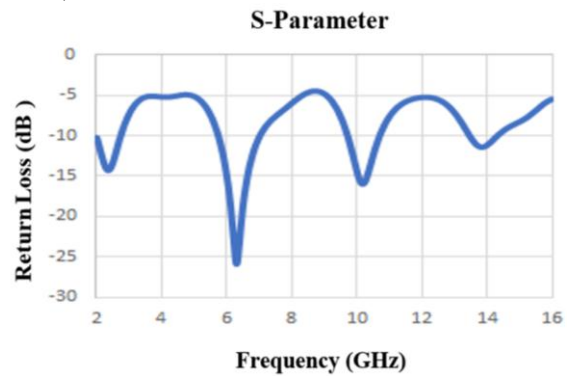
Fig. 10. Simulated Return Loss of the first proposed antenna.

The maximum gain of this antenna design is between 3.7 dBi and 4.8 dBi at the operating bands, as shown below in fig.11.
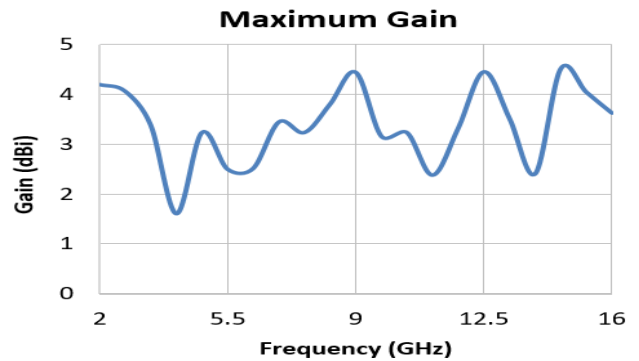
Fig. 11. Simulated Maximum Gain of the first proposed antenna.

Fig. 12 shows the radiation pattern at 2.8 GHz E-plane with a half-power beamwidth of approximately 85°and H-plane is omnidirectional.
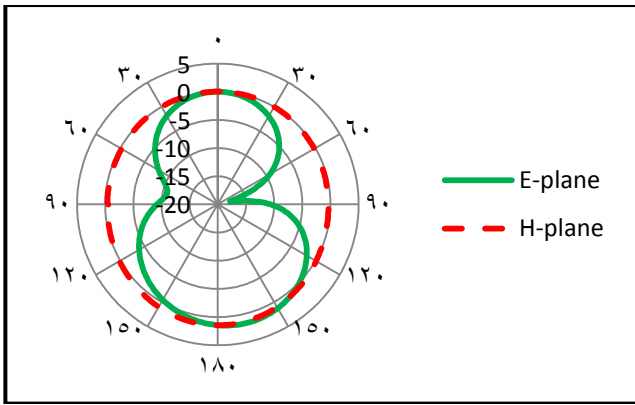
Fig. 12. Simulated Radiation Pattern of the first proposed antenna at 2.8 GHz in E-plane(yz) and H-plane(yx).

b. Second Antenna Results

Fig.13 below shows the S11 simulated result where the change in the ground length resulted in using different frequency bands. The operating frequency bands are from 2.5 GHz to 3.7 GHz, 7 GHz to 8.6 GHz, 10.5 GHz to 12 GHz, and 14.6 GHz to 15.9 GHz.
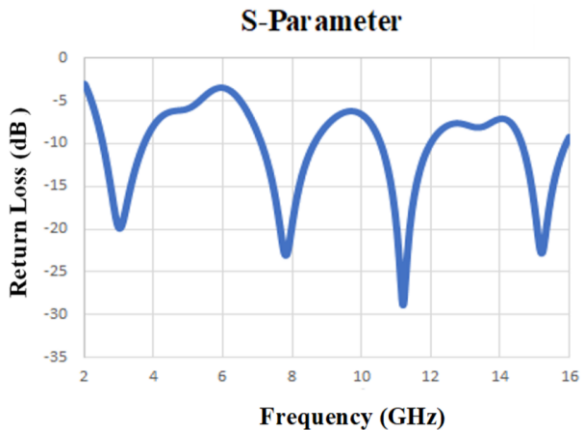
Fig. 13. Simulated Return Loss of the second proposed antenna.

As observed in fig. 14 below, the maximum gain all over the band increased to vary between 4 dBi to 7.22 dBi at the operating frequency bands, and this is due to the change in the antenna ground length.
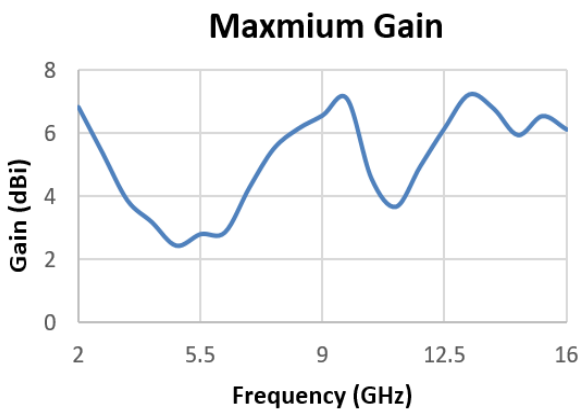
Fig. 14. Simulated Maximum Gain of the second proposed antenna.

Moreover, fig. 15 below shows the farfield radiation pattern at frequency 6.8 GHz with a half-power beamwidth of about 85° and H-plane nearly identical radiation with E-plane.
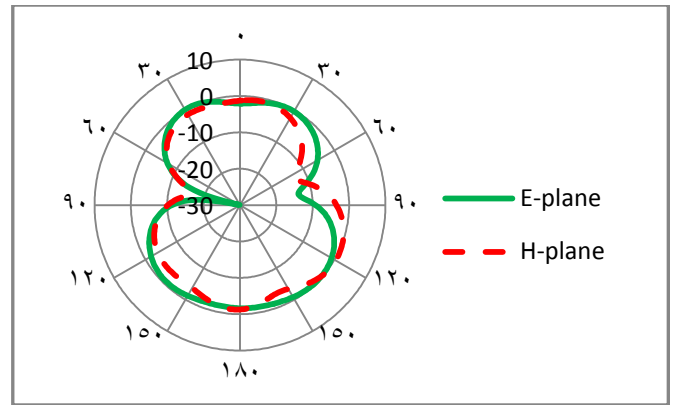
Fig. 15. Simulated Radiation Pattern of the second proposed antenna at 6.8 GHz in E-plane(yz) and H-plane(yx).

c. Third Antenna Results

This design is simulated using two different simulators, which are Ansoft HFSS and CST suite. Each has different solving techniques, which are the Finite Element Method (FEM) and Finite Difference Time Domain (FDTD), respectively. As shown in fig. 16, the antenna is then fabricated using the photolithographic technique at a very low cost due to its simple design and measured using ZVA Network Analyzer of range 10 MHz to 67 GHz. Compared The simulated results to the measuring results show very good agreement, as discussed below.

(a)   (b)
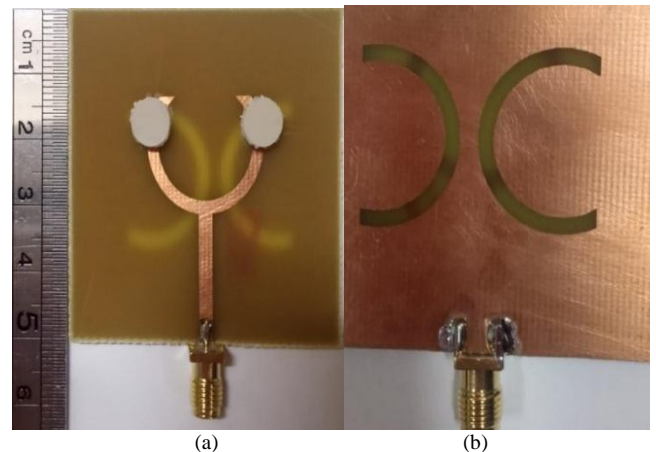
Fig. 16. Third proposed antenna fabrication, (a) front view, and (b) back view.

Fig. 17 below shows the simulated reflection coefficient, S11, results of both simulators compared to the measured results. It can be observed that the simulated results offer perfect matching for frequencies between 6.8 GHz and 7.8 GHz with a bandwidth percentage of 13.8% and a minimum reflection coefficient of about -20 dB at a frequency of 7.25 GHz, whereas between frequencies 10.48 GHz and 35 GHz the bandwidth percentage is87.9% with a minimum reflection coefficient of about -18.8 dB at frequency 12.5 GHz and-34 dB at frequency of 22.4 GHz were achieved.

However, the measured results were very close to the simulated results as the bandwidth percentage for the frequencies between 6.8 GHz and 7.8 GHz is 19%, with a minimum reflection coefficient achieved of about -18.3 dB at a frequency of 7.2 GHz, where it is 73.8% for frequencies

between10.5 GHz to 35 GHz with minimum reflection. coefficient achieved about-23 dB at frequency 14.98 GHz and-34.2 dB at frequency 23.3 GHz. Thus we can say that the measured and simulated results showed a perfect agreement which validated the design accuracy where the antenna can operate in all frequency ranges between 6.8 GHz to 7.8 GHz and between 10.48 GHz to beyond 35 GHz.
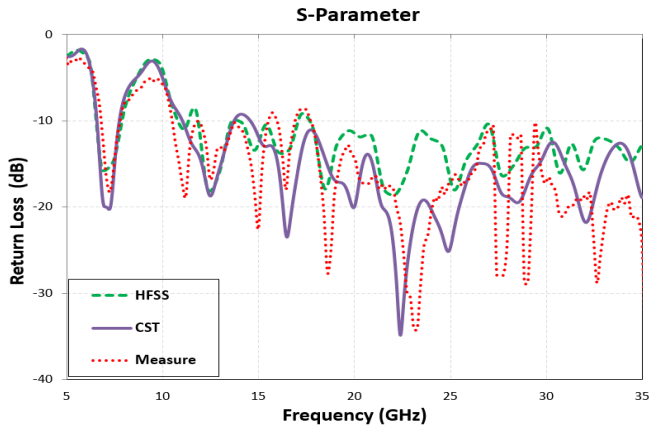
Fig. 17. Simulated and measured reflection coefficients of the CDRA.

Fig. 18 shows the simulated maximum gain by the two simulators (HFSS and CST). The two curves show perfect agreement as the HFSS simulator shows peak gain between 3dBi and 6.7 dBi while the CST simulator shows peak gain between 3.2 dBi and 8.5 dBi along the operating spectrum.
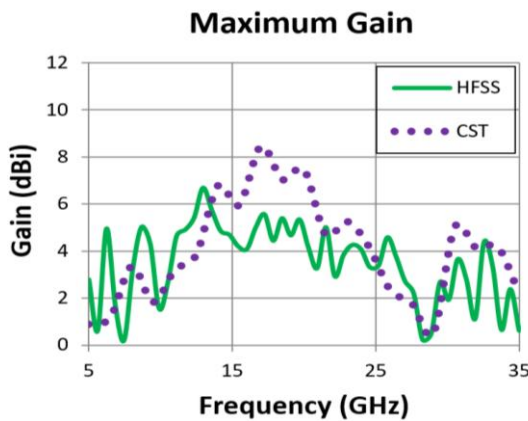
Fig. 18. Simulated Maximum Gain of the third proposed antenna with HFSS and CST simulators.

Fig. 19 (a) shows the simulated radiation pattern in the E-plane and H-plane, and fig. 19 (b) shows the 3D radiation pattern at four different resonating frequencies (7.5 GHz, 20 GHz, 26 GHz, and 33.7 GHz) with half-power beamwidth (HPBW), approximately (77º, 55º, 20º, and 16º) respectively..

In the low and mid frequencies, the radiation pattern has two main directive lobes, which can be suitable for use in many wireless applications, while in the high frequencies, many side lobes are making it capable of use in many different applications.

7.5GHz

20 GHz

26 GHz

33.7 GHz

(a)   (b)
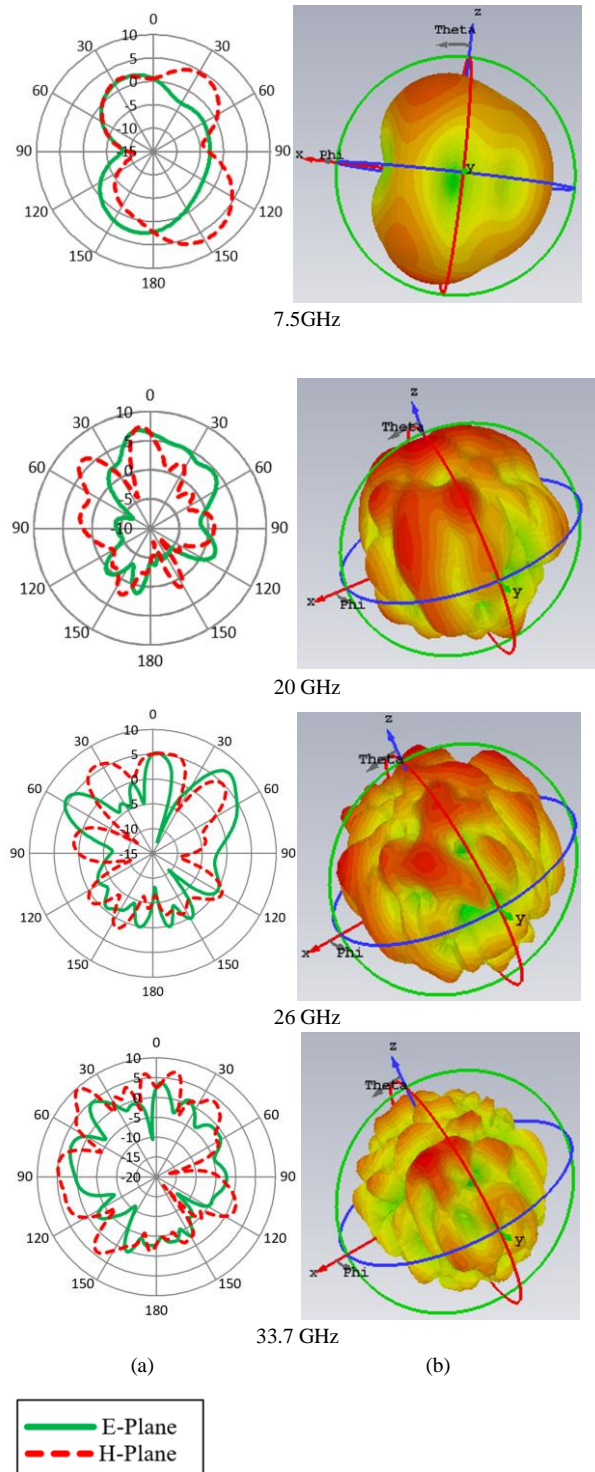
Fig. 19. (a)Simulated E-plane and H-plane at different frequencies, (b) 3D Radiation Pattern

Finally, it is proved that different ground structures for the same radiating antenna affect the bandwidth, resonating frequencies, and antenna gain. Also, using a dielectric resonator with a material different than the used antenna substrate affects the antenna performance as well. Using different ground structures for a CDR antenna, three antennas were designed. Each serves different bandwidths having better performance than the previously reported ones. Table VII below shows a comparison between the three proposed antennas and some recently published research

operating in the same frequency bands. The three proposed antennas can operate in wider bandwidths supporting more applications with comparatively higher gain with more than 2 dBi and easier for fabrication.

V. **Conclusion**

This paper discussed and summarized the effect of different ground structures of the same CDR antenna on the

operating frequency band, radiation pattern, and maximum gain in Table VII below. Each proposed antenna is capable of operating in different frequency bands, but the third CDRA has a wider

TABLE VII. Comparison between the three proposed CDR antennas and the related work

References	Dimension (mm)	Num. of DRs	DR Substrate Used	DR Thickness (mm)	Frequencies (GHz)	Bandwidth (GHz)	Maximum Gain (dBi)
[10]	60 x 45 x 19.5	2	Rogers RT 5880 $\varepsilon_r = 2.2$ and $\tan\delta = 0.0009$	19	4.8-9.66	67.5%	N/A
[11]	16 x 8.5 x 10	1	$\varepsilon_r = 9.6$	8.3	3.1-12.1	N/A	unstable
[14]	33 x 38 x 7.524	3	$\varepsilon_r = 10$ and $\tan\delta = 0.0002$	6	2.54-3.22, 4.06-5.04, 6.04-13.64	137%	5.9
[15]	N/A x N/A x 3.9	2	Silicon-nitrate ($\varepsilon_r = 7$) & Rogers TM-6 ($\varepsilon_r = 6$)	2.3	26.9	25.1-30.1	6.5
[24]	60 x 60 10.508	1	$\varepsilon_r = 10$	10	3.85 , 7.85	10%, 10%	6.26
Proposed Antenna 1	50 x 50 x 3.6 **(Ground = 50 x 16.6)**	2	Rogers RT/Duroid 6010LM $\varepsilon_r = 10.2$ and $\tan\delta = 0.0023$	2	2.4, 6.6, 10.4, 13.9	2 – 2.8, 5.7 – 7.2, 9.7 – 10.7, 13.4 – 14.3	4.8
Proposed Antenna 2	50 x 50 x 3.6 **(Ground = 50 x 19.6)**	2	Rogers RT/Duroid 6010LM $\varepsilon_r = 10.2$ and $\tan\delta = 0.0023$	2	3.1, 7.8, 11.2, 15.1	2.5 – 3.7, 7 – 8.6, 10.5 – 12, 14.6 – 15.9	7.22
Proposed Antenna 3	50 x 50 x 1.6 **(Ground = 50 x 50)**	2	Rogers RT/Duroid 6010LM $\varepsilon_r = 10.2$ and $\tan\delta = 0.0023$	2	7.5, 11.5, 12.5, 15, 16.8, 18.6, 20, 23, 26, 29, 33.7	6.8 – 7.8, 10.5 – 35	8.5

frequency range extending from 6.8 GHz to 7.8 GHz and from 10.5 GHz to beyond 35 GHz with a peak gain of 8.5 dBi. Proved these results by using two different simulators (HFSS and CST) with different solving techniques (FEM and FDTD, respectively). Compared them to the measuring results showing perfect agreement making it a good candidate for use in WiMAX, C-band, X-band, Ku-band, 5G, and modern millimeter wave wireless technology applications.

REFERENCES

[1] S. Gupta, A. Sharma, G. Das, R. K. Gangwar, and M. Khalily, "Wideband Circularly Polarized Dielectric Resonator Antenna Array with Polarization Diversity," *IEEE Access*, vol. 7, pp. 49069–49076, 2019, doi: 10.1109/ACCESS.2019.2909581.

[2] A. Gupta and R. K. Gangwar, "Compact two-element cylindrical dielectric resonator antenna array for quad-band applications," *2018 3rd Int Conf Microw Photonics, ICMAP 2018*, vol. 2018-Janua, no. Icmap,

pp. 1–2, 2018, doi: 10.1109 /ICMAP.2018.8354649.

[3]   A. Zaidi, A. Baghdad, A. Ballouk, and A. Badri, "Performance enhancement of an inset fed circular microstrip patch antenna using periodic defected ground structure and EBG superstrates for applications in the millimeter wave band," *Int J Commun Antenna Propag*, vol. 8, no. 2, pp. 116–122, 2018, doi: 10.15866/irecap.v8i2.12798.

[4]   J. K. Xu, L. Y. Feng, M. Wang, M. J. Adamu, Y. Liu and W. S. Ji, "Millimeter-wave Dual Rectangular Dielectric Resonator Antenna with Bidirectional Radiation Pattern," 2020 IEEE Asia-Pacific Microwave Conference (APMC), 2020, pp. 595-597, doi: 10.1109/APMC47863.2020.9331619.

[5]   A. Sarkar and S. Lim, "60 GHz compact larger beam scanning range PCB leaky-wave antenna using HMSIW for millimeter-wave applications," *IEEE Trans Antennas Propag*, vol. 68, no. 8, pp. 5816–5826, 2020, doi: 10.1109/TAP.2020.2983784.

[6]   N. M. Rashad and A. A. M. Khalaf, "Modified Design and Fabrication of a broadband Millimeter-Wave Ankh-Key Antenna for 5G and Next Generations Applications," *Proc 2020 Int Conf Innov Trends Commun Comput Eng ITCE 2020*, no. February, pp. 322–325, 2020, doi: 10.1109/ITCE48509.2020.9047793.

[7]   FCC Opens 6 GHz Band to Wi-Fi and Other Unlicensed Uses, https://www.fcc.gov/document/fcc-opens-6-ghz-band-wi-fi-and-other-unlicensed-uses-0, April, 2020.

[8]   A. Omar and A. Omar, "A Sub-6 GHz Antenna Array with Reduced Mutual Coupling Using Optimized Defected Ground Structure for 5G Testbeds," 2021 44th International Conference on Telecommunications and Signal Processing (TSP), 2021, pp. 239-243, doi: 10.1109/TSP52935.2021.9522639.

[9]   A. Petosa, Dielectric Resonator Antenna Handbook. Norwood, MA: Artech House, 2007.

[10]   R. -Y. Li, Y. -C. Jiao, Y. -X. Zhang, H. -Y. Wang and C. -Y. Cui, "A Wideband MIMO Triangular Dielectric Resonator Antenna with A Simple Decoupling Structure," 2020 9th Asia-Pacific Conference on Antennas and Propagation (APCAP), 2020, pp. 1-2, doi: 10.1109/APCAP50217.2020.9246103.

[11]   B. Liu, B. Yu, Q. Jinghui and K. Yao, "Sharply Defined UWB Rectangular Dielectric Resonator Antenna," 2020 IEEE International Symposium on Antennas and Propagation and North American Radio Science Meeting, 2020, pp. 325-326, doi: 10.1109/IEEECONF35879.2020.9330068.

[12]   E. Baldazzi et al., "A High-Gain Dielectric Resonator Antenna With Plastic-Based Conical Horn for Millimeter-Wave Applications," in IEEE Antennas and Wireless Propagation Letters, vol. 19, no. 6, pp. 949-953, June 2020, doi: 10.1109/LAWP.2020.2984565.

[13]   Y. Yu, W. -W. Yang and J. -X. Chen, "A Low-profile Wideband Dielectric Resonator Antenna Suitable for Beam-forming Applications," 2020

IEEE Asia-Pacific Microwave Conference (APMC), 2020, pp. 607-609, doi: 10.1109/APMC47863.2020.9331717.

[14]   M. Abedian, M. Khalily, S. Danesh, P. Xiao and R. Tafazolli, "A Novel Dual Band-notched UWB Printed Monopole Loaded with Dielectric Resonators," 2021 15th European Conference on Antennas and Propagation (EuCAP), 2021, pp. 1-5, doi: 10.23919/EuCAP51087.2021.9411496.

[15]   M. U. K. Asadullah, M. S. Sharawi and A. Shamim, "Circularly Polarized Dielectric Resonator Antenna for mm- Wave Applications," 2021 International Applied Computational Electromagnetics Society Symposium (ACES), 2021, pp. 1-2, doi: 10.1109/ACES53325.2021.00193.

[16]   L. Guo, C. Zhou, H. Li, P. Chu and W. W. Yang, "Low-Profile and Broadband Dielectric Resonator Antenna Using Higher-Order Modes," in IEEE Antennas and Wireless Propagation Letters, vol. 20, no. 10, pp. 1988-1992, Oct. 2021, doi: 10.1109/LAWP.2021.3101648.

[17]   M. Rad, N. Nikkhah, B. Zakeri and M. Yazdi, "Wideband Dielectric Resonator Antenna With Dual Circular Polarization," in IEEE Transactions on Antennas and Propagation, vol. 70, no. 1, pp. 714-719, Jan. 2022, doi: 10.1109/TAP.2021.3098516.

[18]   H. Tang, X. Deng and J. Shi, "Wideband Substrate Integrated Differential Dual-Polarized Dielectric Resonator Antenna," in IEEE Antennas and Wireless Propagation Letters, vol. 21, no. 1, pp. 203-207, Jan. 2022, doi: 10.1109/LAWP.2021.3125100.

[19]   Z. Zhu et al., "A Compact Pattern Reconfiguration Antenna Based on Multimode Plane Spiral OA," in IEEE Transactions on Antennas and Propagation, vol. 69, no. 2, pp. 1168-1172, Feb. 2021, doi: 10.1109/TAP.2020.3010954.

[20]   S. Varghese, A. Parambil, A. M. Baby and J. P M, "High Gain Dual-Band Waveguide Fed Dielectric Resonator Antenna," in IEEE Antennas and Wireless Propagation Letters, doi: 10.1109/LAWP.2021.3124225.

[21]   J. Liu et al., "A Low Profile, Dual-Band, Dual-Polarized Patch Antenna With Antenna-Filter Functions and Its Application in MIMO Systems," in IEEE Access, vol. 9, pp. 101164-101171, 2021, doi: 10.1109/ACCESS.2021.3096969.

[22]   M. Boyuan, J. Pan, S. Huang, D. Yang and Y. Guo, "Wide-Beam Dielectric Resonator Antennas Based on the Fusion of Higher-Order Modes," in IEEE Transactions on Antennas and Propagation, vol. 69, no. 12, pp. 8866-8871, Dec. 2021, doi: 10.1109/TAP.2021.3090840.

[23]   X. -H. Ding, W. -W. Yang, W. Qin and J. -X. Chen, "A Broadside Shared-aperture Antenna for (3.5, 26) GHz Mobile Terminals with Steerable Beam in Millimeter Wave Band," in IEEE Transactions on Antennas and Propagation, doi: 10.1109/TAP.2021.3118817.

[24]   P. Gupta, D. Guha and C. Kumar, "Dual-Mode
       Cylindrical DRA: Simplified Design With Improved
       Radiation and Bandwidth," in IEEE Antennas and
       Wireless Propagation Letters, vol. 20, no. 12, pp.
       2359-2362, Dec. 2021, doi:
       10.1109/LAWP.2021.3110875.

[25]   Zaki, A., Hamad, E., Abouelnaga, T., & Elsadek, H.
       (2022). Design of ultra-compact ISM band
       implantable patch antenna for bio-medical
       applications. International Journal of Microwave and
       Wireless Technologies, 1-10.
       doi:10.1017/S1759078721001732.